

How Do Inhibitors Mitigate Corrosion in Oil-Water Two Phase Flow Beyond Lowering the Corrosion Rate?

Chong Li, Sonja Richter, and Srdjan Nesic
Institute for Corrosion and Multiphase Technology
Ohio University
342 West State Street
Athens, OH 45701

ABSTRACT

Corrosion inhibitors are commonly used to mitigate corrosion in oil and gas pipelines and the choice of inhibitor for a particular oil field depends on the conditions of the field (oil chemistry, water chemistry, temperature, etc.). In order to find the optimum formulation for each field condition, extensive laboratory tests are carried out which include corrosion inhibitor performance, foaming, and emulsification, to name a few. When it comes to measuring the inhibition efficiency of the corrosion inhibitor formulation, the focus is on the inhibition from the water phase. However, corrosion inhibitors can have an additional advantage of altering the wettability of the steel surface from hydrophilic (water wet) to hydrophobic (oil wet) by forming a hydrophobic adsorption layer on the steel surface. In the current work, the ability of corrosion inhibitors to alter the wettability of the steel is investigated by measuring the static contact angle in a goniometer, as well as the dynamic wetting with a small scale flow apparatus, called a doughnut cell, especially designed for this purpose. The doughnut cell makes it possible to measure the water and oil wetting of a steel surface using flush mounted conductivity pins that detect whether water (conductive fluid) or oil (nonconductive fluid) are covering the surface. The two generic inhibitors tested here, a quaternary ammonium chloride and a fatty amine, lowered the corrosion rate, altered the surface wetting from hydrophilic (mostly water wet) to hydrophobic (mostly oil wet) and lowered the oil-water interfacial tension, facilitating water entrainment in the oil. A doughnut cell was used to map out how an inhibitor can increase the oil wetting regime for a given water cut. It is a practical tool that can be used to help optimizing the inhibitor dosage and maximizing its value. It can also be used in new field development, where enhanced oil wetting could be factored into the corrosion allowance calculation.

KEY WORDS: corrosion inhibitors, CO₂ corrosion, wettability, carbon steel, adsorption

INTRODUCTION

Adsorption and efficiency of corrosion inhibitors have been extensively researched for industrial application in the oil and gas industry starting in the middle of the 20th century most notably with the work of Hackerman starting in 1949¹. Publication in the literature on corrosion inhibitors has steadily been increasing and in the last 6 years has reached more than 500 publications a year. The research is nearly exclusively focused on the action of the corrosion inhibitor from the water phase only, ignoring the effect of the oil phase. However, the oil phase can enhance the performance of the corrosion inhibitor, as well as produce added protection by increased oil wetting and increased water entrainment.

A handful of researchers have looked at the effect of corrosion inhibitors on the steel surface wettability and/or interfacial tension. McMahon¹ observed how adding oleic imidazoline (OI) to the oil phase rendered the steel surface completely hydrophobic resulting in droplets of water simply rolling of a steel disc. He also saw a drastic decrease in the oil-water interfacial tension with the addition of oleic imidazoline, reducing it to less than 1 mN/m with a concentration of only 10 ppm of OI.

Foss, et al. have investigated the effect of corrosion inhibitors on the wettability of corroded steel surface,² iron carbonate covered steel surface³ and ferric covered steel surface.⁴ Both oleic imidazoline and phosphate ester were able to alter the wettability in water-in-oil contact angle measurements from hydrophilic to hydrophobic increasing the oil wetting, while cetyltrimethylammonium bromide (CTAB) made the surface increasingly water wet. However, for the oil-in-water contact angle measurement, only the oxidized ferric corrosion product layer became oil wet in the presence of an inhibitor.⁴ The authors also concluded that the corrosion inhibition of the surface could be greatly enhanced with an exposure to the oil phase due to modification of the inhibitor film.

Schmitt and Stradmann⁵ conducted contact angle measurements by placing oil and water droplets on carbon steel specimens in a high pressure test apparatus. The tests were performed under 75 and 80 °C and 5 bar CO₂. The testing fluids were different crude oils, a synthetic oil and brine with surfactants (inhibitors and demulsifiers) added into the system. The contact angle measurements were made on the clean surface and pre-corroded (6, 24, 48 and 72 hours) surface. It was found that a clean carbon steel surface and a pre-corroded surface covered with FeCO₃ scale both show hydrophilic wetting property. The addition of quaternary ammonium inhibitor under FeCO₃ scale formation conditions resulted in a hydrophilic surface, however fatty amine and imidazoline based inhibitors produced a hydrophobic surface.

The current paper seeks to separate and emphasize the multifaceted roles of corrosion inhibitors which are not only acting to reduce corrosion directly but also to facilitate the entrainment of water and render the surface hydrophobic (oil wet).

EXPERIMENTAL MATERIALS AND PROCEDURES

Materials

Two generic inhibitor compounds were tested: a quaternary ammonium chloride (“quat”) and a fatty amine compound. The composition of the quaternary ammonium chloride solution, included methanol as solvents, is given in Table 1, and the composition of the generic fatty amine corrosion inhibitor solution is given in Table 2 with acetic acid and methanol used as solvents for the fatty amine compound. The model oil was LVT200^{TM*} with the properties listed Table 3. LVT200 is a clear, light

* Trade name

©2013 by NACE International.

Requests for permission to publish this manuscript in any form, in part or in whole, must be in writing to NACE International, Publications Division, 1440 South Creek Drive, Houston, Texas 77084.

The material presented and the views expressed in this paper are solely those of the author(s) and are not necessarily endorsed by the Association.

paraffinic distillate consisting of straight chain hydrocarbon (C9 – C16) with C14 being the most common fraction. It does not contain any impurities which would affect the corrosion rate.⁶ Composition of the of the UNS G10180 steel is given in Table 4.

Table 1
Composition of quaternary ammonium chloride inhibitor package

Substance	Weight (%)
Quaternary ammonium chloride	60 – 80
Methanol	10 – 30

Table 2
Composition of fatty amine inhibitor package

Substance	Weight (%)
Fatty amine compound	60 – 80
Acetic acid	10 – 30
Methanol	5 - 10

Table 3
Properties of the model oil used in the research

Property	Parameter	Value
Density	ρ	825 kg/m ³
Viscosity @25°C	μ	2.0 mPa.s
Interfacial Tension	σ	40 mN/m
Oil-in-Water Contact Angle	θ	73°

Table 4
Elemental composition of the mild steel (UNS G10180) sample used as a rotating cylinder electrode (RCE).

Elements	Weight (%)
C	0.21
Si	0.38
P	0.09
S	0.05
Mn	0.05
Al	0.01
Fe	Balance

Procedure for Corrosion Inhibition Measurements

The corrosion testing was performed in a 2 L glass cell using three electrodes: a rotating cylinder made out of UNS G10180 pipeline steel (see Table 4)) with an exposed surface area of 5.4 cm² as the working electrode, a silver/silver-chloride (Ag/AgCl) as the reference electrode located in a Luggin capillary tube and a platinum ring as the counter electrode. The linear polarization resistance (LPR) technique was used to measure the corrosion rate.

The glass cell including the Ag/AgCl reference electrode and the platinum counter electrode was filled with 2.0 L of 1.0 wt% NaCl solution, deoxygenated by purging with CO₂ for 1.5 – 2 hours to reach oxygen concentration below 25 ppb. The equilibrium pH of the test solution is 3.8 – 3.9 and was adjusted to pH 5.0 by adding a deoxygenated sodium bicarbonate (NaHCO₃) solution. The working electrode was polished with 400 and 600 grit silicon carbide paper using isopropyl alcohol as the cooling fluid. After polishing, the working electrode was cleaned in an ultrasonic bath with isopropyl alcohol and air dried with a blower. It was then mounted on the rotating electrode holder and inserted into the glass cell maintaining a rotation speed of 1000 rpm. The temperature of the test was maintained at 25 °C.

A potentiostat was connected to the three electrodes and the open circuit potential was first monitored for 5 – 10 minutes until it became stable. Linear polarization resistance (LPR) technique was conducted at 30 minutes interval throughout the test to measure the corrosion rate. The polarizing

range was ± 5 mV from the open circuit potential with scanning rate of 0.125 mV/s. The measured polarization resistance, R_p , was compensated with the solution resistance, R_s , measured by the electrochemical impedance spectroscopy (EIS) technique. The B-value for calculating the corrosion rate from LPR measurement was evaluated with weight loss and potentiodynamic sweeps and a value of 21 mV/decade was obtained for measurements without an inhibitor as well as with quaternary ammonium chloride. However, for the fatty amine measurements the B-value was determined to be 31 mV/decade.⁷

The corrosion inhibitor was introduced into the cell with a syringe 1.5 hour after the working electrode has been exposed to the solution and separate experiments were made for inhibitor concentrations ranging from 0 – 200 ppm. Two series of glass cell experiments were conducted: For the so called "pure corrosion inhibition" tests, only the brine phase was present in the glass cell. For the "direct oil wet" tests, the paraffinic model oil was added on top of the brine (in 1:9 volumetric ratio) and the working electrode was periodically lifted up into the oil phase and left there for 5 minutes rotating at 1000 rpm and then returned to the water phase for electrochemical measurements. The inhibitor concentration is calculated based on the total liquid volume (2 L) and the inhibition efficiency (IE) is calculated according to Equation (1) as a function of the inhibited ($CR_{inhibited}$) and uninhibited ($CR_{uninhibited}$) corrosion rates.

$$IE = \frac{CR_{uninhibited} - CR_{inhibited}}{CR_{uninhibited}} \quad (1)$$

Procedure for Interfacial Tension Measurements

A CSC⁺ DuNouy tensiometer was used to measure the changes of oil-water interfacial tension due to the addition of an inhibitor. The tensiometer has a platinum wire ring, which is immersed in the water phase. The oil phase is slowly added on top of the water phase. The platinum ring is pulled up and when it breaks through the oil-water interface, the required force in units of dyne/cm (equal to the S.I. unit mN/m) can be read directly from the dial of the tensiometer.

Deionized water with 1 wt% NaCl was deoxygenated by purging CO₂ gas in a 500-mL breaker for 1 hour and is adjusted to pH 5.0 by adding NaHCO₃. To control the water chemistry during the addition of an inhibitor, a plastic glove bag with CO₂ gas continuously purging was used. The corrosion inhibitor was added to a test tube which contained 15-mL oil and 15-mL brine (deionized water with 1 wt% NaCl) with the concentration of inhibitor calculated based on the total volume of liquid. After the addition of an inhibitor, the test tube was shaken for a few minutes and then set still for a period of 1 day for the inhibitor to partition. At the end of the partitioning period the oil and the water were transferred by syringes to a glass container for tensiometer measurements.

Procedure for Contact Angle Measurements

The contact angle measurements were conducted with the custom built goniometer, shown in Figure 1, which can measure both: (a) the contact angle of an oil droplet sitting on a steel surface in a continuous brine phase (oil-in-water contact angle) and (b) the contact angle of a water droplet suspended on a steel surface in a continuous oil phase (water-in-oil contact angle). Since both of the inhibitors described in this study were predominantly water soluble, the results presented below focus on the oil-in-water contact angle (see Figure 2). The contact angle is always measured through the water phase and a larger contact angle ($>90^\circ$) indicates a hydrophobic (preferentially oil wet) surface, while a low contact angle ($<90^\circ$) indicates a hydrophilic (preferentially water wet) surface.

* Trade name

A carbon steel coupon was polished and placed on a Teflon^{TM†} sample holder inside the goniometer vessel. The videos of the droplet were analyzed by an image analyzing software and the contact angle θ calculated according to Equation 2, where R is the radius of the droplet and L is the length of the contact line, both of which are provided by the image analyzing software in the unit of pixels.

$$\theta = 180 - \arcsin\left(\frac{L}{2R}\right) \cdot \frac{180}{\pi} \quad (2)$$

For the contact angle tests the vessel of the goniometer was filled with 500 mL of deionized water with 1 wt% NaCl. A sparger was inserted into the liquid to purge CO₂ gas for deoxygenation. The pH of the brine phase was adjusted to 5.0 with NaHCO₃. A flat API 5L X65 carbon steel sample was polished with 400- and 600-grit SiC paper, washed with isopropanol and dried with a hot air blower. After the sample was immersed into the water phase, an oil droplet was placed underneath the surface using a 10- μ L syringe. A baseline test (without inhibitor) was carried out first and then the corrosion inhibitor was injected into the continuous water phase measurements taken and the concentration was increased stepwise.

Procedure for Dynamic Wetting Measurements

A benchtop apparatus, called *doughnut cell*, was developed to simulate oil-water pipe flow on a small scale. The main purpose of the doughnut cell was to determine the occurrence of oil vs. water wetting at the bottom of a pipe, at a given water cut and oil velocity and it can also be used for corrosion rate measurements. An image of the equipment can be seen in Figure 3a and a sketch of the cross sectional view of the rectangular shaped channel where the oil and water are flowing is seen in Figure 3b. Oil and water are introduced into the channel at a given ratio and the flow is introduced by the top lid rotating. Due to direct contact, the lid shears the oil phase, which in turn shears and possibly entrains the water phase. Series of conductivity pins⁸ are flush mounted at the stainless steel bottom of the channel, to detect whether water or oil is wetting the bottom.

Since the channel has a rectangular cross section, computational fluid dynamics (CFD) modeling was used to optimize the geometry of the cross section with regards to secondary flow which might disrupt the water entrainment by the oil phase. The width of the annulus is 46 mm and it sits between a 0.46 m OD (wall thickness 6 mm) and a 0.35 m OD (wall thickness 2.5 mm) acrylic cylinders. The height of the annulus is adjustable and is set here at 70 mm, which results in a working volume of 4.2 liters. Since the cross section of the channel is rectangular, the hydraulic diameter is calculated according to Equation (3) with H being the height [mm] and W the width [mm] of the annulus.

$$D_H = \frac{2 \cdot H \cdot W}{H + W} \quad (3)$$

A Pitot tube was used to measure the oil phase velocity during testing. It was inserted into the cell through the bottom and used for measuring *in situ* circumferential velocity of the oil phase. The pitot tube was connected to a differential pressure transducer. The measured differential pressure, Δp (psi), can be converted to fluid velocity, u (m/s) according to Bernoulli's equation (Equation 4), in which 6894.76 is a unit conversion factor for pressure from psi to Pa and ρ_{fluid} is the density of the fluid (kg/m³), which in this case is the density of the model oil (825 kg/m³).

$$u = \sqrt{\frac{2 \cdot \Delta p \cdot 6894.76}{\rho_{fluid}}} \quad (4)$$

* American Petroleum Institute, 1220 L Street NW, Washington, DC 20005, USA

©2013 by NACE International.

Requests for permission to publish this manuscript in any form, in part or in whole, must be in writing to NACE International, Publications Division, 1440 South Creek Drive, Houston, Texas 77084.

The material presented and the views expressed in this paper are solely those of the author(s) and are not necessarily endorsed by the Association.

The volume of water and oil which are placed into the channel are determined based on the desired water cut. Water is first poured into the cell from the top and then the oil is added. The measurement point for the Pitot tube is set in the middle of the oil phase. The test starts at the low lid rotational speed which gives low oil velocity and a conductivity pin measurement is carried out. The rotation is then stopped and the oil and water are allowed to separate before the rotation speed is set to give a higher velocity. This is repeated until all the water from the bottom is entrained and oil wetting has been detected by the conductivity pins. The whole procedure is repeated again for a different water cut until a full phase wetting map has been created.

All the different pieces of equipment used in the present research (glass cell, tensiometer, goniometer and doughnut cell) were thoroughly cleaned after each test with tap water, DI water and isopropyl alcohol in succession, to avoid inhibitor cross-contamination.

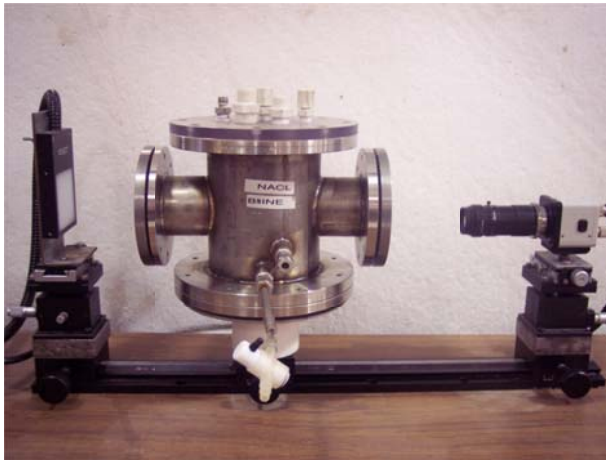


Figure 1: The vessel of the goniometer is situated in between a video camera on the right, which records the contact angle, and a backlight on the left.

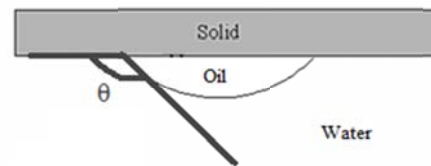


Figure 2: Sketch of the oil-in-water contact angle, θ . Larger the contact angle, the more hydrophobic the surface becomes.

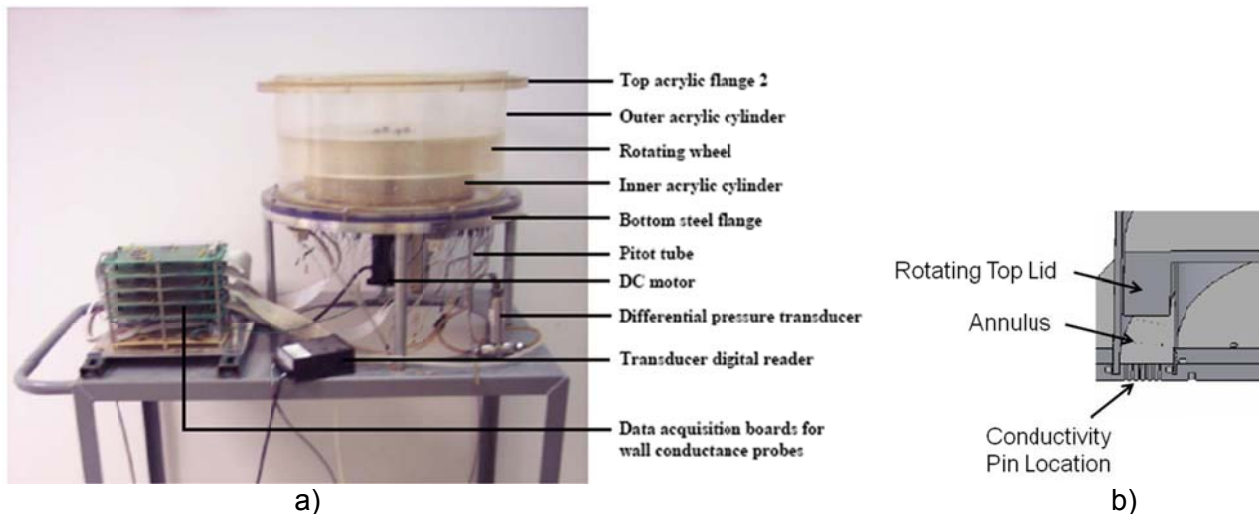


Figure 3: a) Doughnut cell apparatus used for dynamic wettability measurements in oil-water flow. b) Cross section of the annulus of the doughnut cell, including location of the rotating top and the conductivity pins.

RESULTS AND DISCUSSION

Corrosion Inhibition

Figure 4a shows the pure corrosion inhibition (from water phase only) obtained by adding increasing concentrations of quaternary ammonium chloride to the water phase. The corrosion rate steadily decreases as the concentration of inhibitor increases and a fairly high concentration of 200 ppm is needed to produce a significant corrosion inhibition within the first 5 hours of testing. On the other hand, the fatty amine inhibitor (Figure 4b) can produce a significant corrosion inhibition at 5 hours with as little as 5 ppm concentration. Inhibited corrosion rate and inhibition efficiency (according to Equation 1) are directly compared in Figure 5, and the difference in the performance of the two inhibitor packages at the same concentration is evident. Although the corrosion inhibition at high concentrations (200 ppm) is similar for both the inhibitors (ca. 95%), fatty amine reaches high inhibition efficiency at much lower concentration compared with quaternary ammonium chloride.

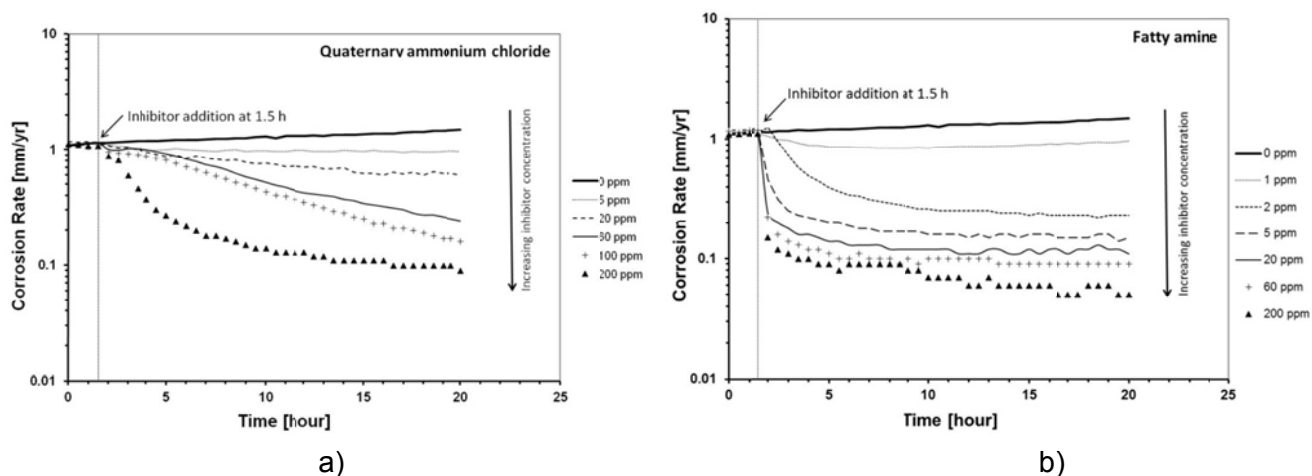


Figure 4: Inhibition of corrosion after the addition of a) quaternary ammonium chloride and b) fatty amine at various concentrations. The vertical dotted line at 1.5 hours indicates the addition of the inhibitor to the water phase.

Figure 6 shows the result of exposing the corrosion sample periodically to a model oil (*direct oil wet*). In the case of quaternary ammonium chloride (Figure 6a), there is no effect of exposing the sample to the oil phase, neither at 5 ppm concentration as shown in the Figure 6a, nor at any other higher concentration (not shown here). However, in the case of the fatty amine inhibitor (Figure 6b), there is a dramatic drop of the corrosion rate as the sample is exposed to the oil phase. One needs to recall that the model oil is composed of straight chain hydrocarbon molecules, which do not have an affinity to adsorb on the steel surface, and do not directly affect the corrosion process⁶. After only a short exposure (5 min) to the inert model oil (containing some inhibitor), the corrosion rate drops from 0.75 mm/yr to 0.37 mm/yr and settles at 0.2 mm/yr. A subsequent exposure to the oil phase results in a slight decrease in the corrosion rate to 0.15 mm/yr, but further exposing the sample to the oil phase does not affect the corrosion rate.

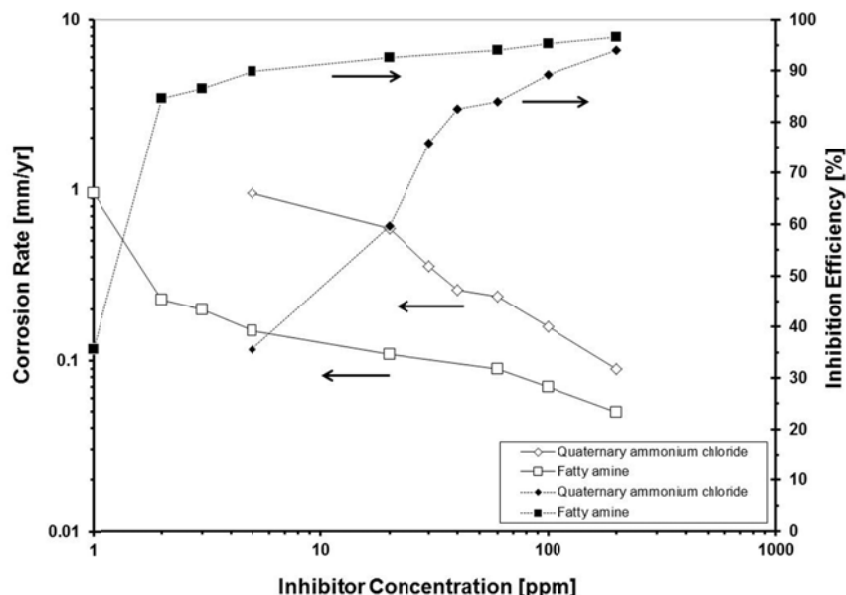


Figure 5: Comparison of the corrosion inhibition and the inhibition efficiency of the two inhibitor packages.

The quicker and more efficient inhibition by the fatty amine inhibitor compared to quaternary ammonium chloride in these tests suggests that the fatty amine inhibitor more readily forms a self-assembled monolayer at the steel surface with the hydrophilic head group adsorbed on the surface and the hydrophobic tail pointed to the bulk solution (Figure 7a). The tails of fatty amine molecules line up and can provide a barrier that impedes water molecules, as well as the dissolved corrosive species, to reach the steel surface. When the steel surface is subsequently exposed to the oil phase, the alkane molecules (C12 – C17) that make up the oil phase can line up with the hydrocarbon tails of the fatty amine molecules on the surface (Figure 7b) and thus strengthening the “monolayer” even further (hence the drop in corrosion rate). The impressive efficiency of the fatty amine inhibitor seems to be less due to its ability to adsorb on the surface but rather due to the inhibitor’s ability to create a strong protective layer on the surface.

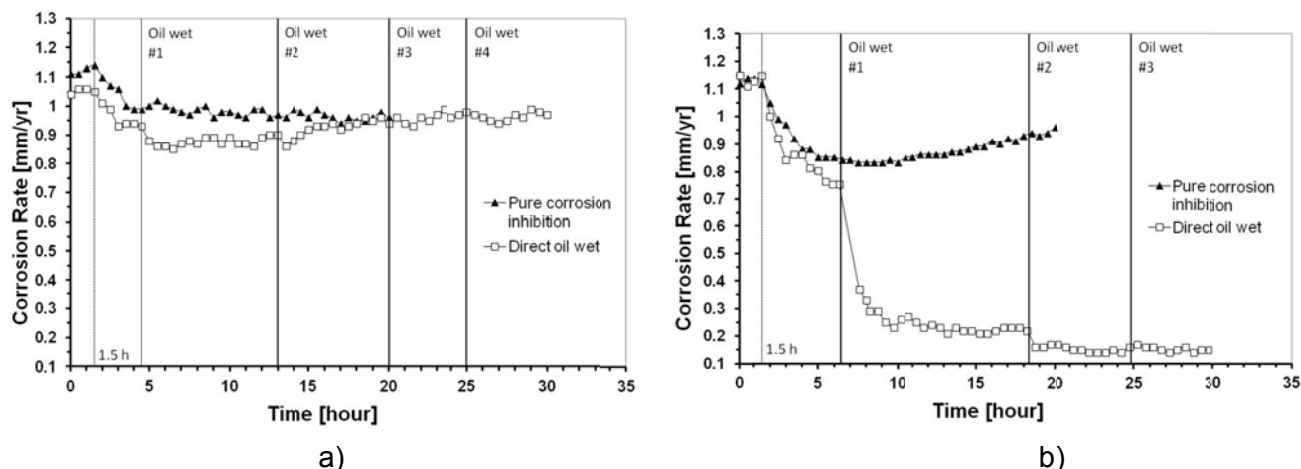


Figure 6: Direct oil wet test for a) quaternary ammonium chloride at 5ppm concentration and b) fatty amine inhibitor at 1 ppm concentration. The dotted line at 1.5 hour notes when the inhibitor was added to the water phase and the solid lines note when the sample was exposed to the oil phase.

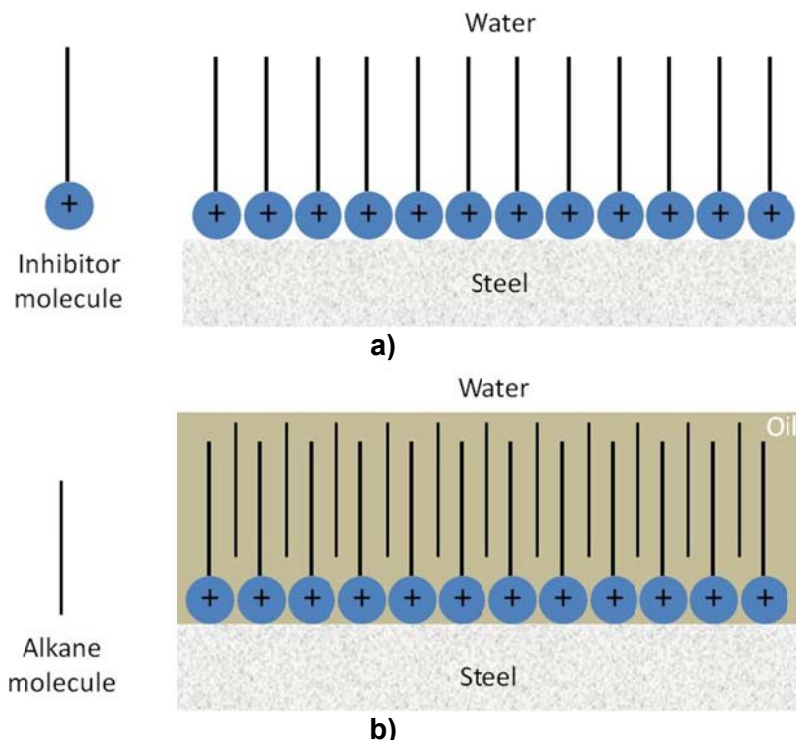


Figure 7: Illustration of a) monolayer composed of inhibitor molecules adsorbed from the water layer, b) monolayer of adsorbed inhibitor after exposure to oil, where the oil molecules (e.g., alkanes) will pack between the tails of the inhibitor molecules to form a protective oil barrier impeding water molecules to reach the steel surface.

Interfacial Tension

Corrosion inhibitors do not only gather at the steel-water interface. They can also gather at the oil-water interface and subsequently lower the interfacial tension. The interfacial tension between the model oil and the water phase was measured to be 40 mN/m. Figure 8a shows that even at low inhibitor concentrations the interfacial tension can be significantly reduced. Only 1 ppm of fatty amine is enough to lower the interfacial tension to 21.9 mN/m. The interfacial tension drops fairly rapidly for the lowest concentrations of inhibitor but then start to level off as the concentration is increased further. The concentration at which the interfacial tension starts to level off is called the critical micelle concentration (CMC) and denotes the concentration at which the oil-water interface becomes saturated with inhibitor and micelles start to form in the liquid phase. For fatty amine the CMC was measured to be 3 ppm and for quaternary ammonium chloride the CMC was 5 ppm. The interfacial tension at the CMC is about 5 mN/m for both of the inhibitors.

Since the water phase is heavier than the oil phase, the water phase tends to settle at the bottom of the pipe, but sufficient turbulent energy of the flow can overcome the gravitational effect and entrain the water. In the process of entraining the water, it is broken up into droplets and the efficiency of this process depends on the interfacial tension. Therefore, lower interfacial tension makes water droplet breakup easier and facilitates the entrainment of water. To illustrate this effect, which is hard to measure directly, a water wetting model⁹ is used to predict the transition between oil and water wetting, depending on the oil properties, geometric factors and flow rates of oil and water. The pipe diameter used for the simulation here is the hydraulic diameter of the rectangular cross section doughnut cell channel (calculated to be 0.0555 m). The resulting transition from water to oil wetting is shown in Figure 8b for water cuts less than 20%. The total liquid velocity refers to the combined superficial velocity of oil and water.

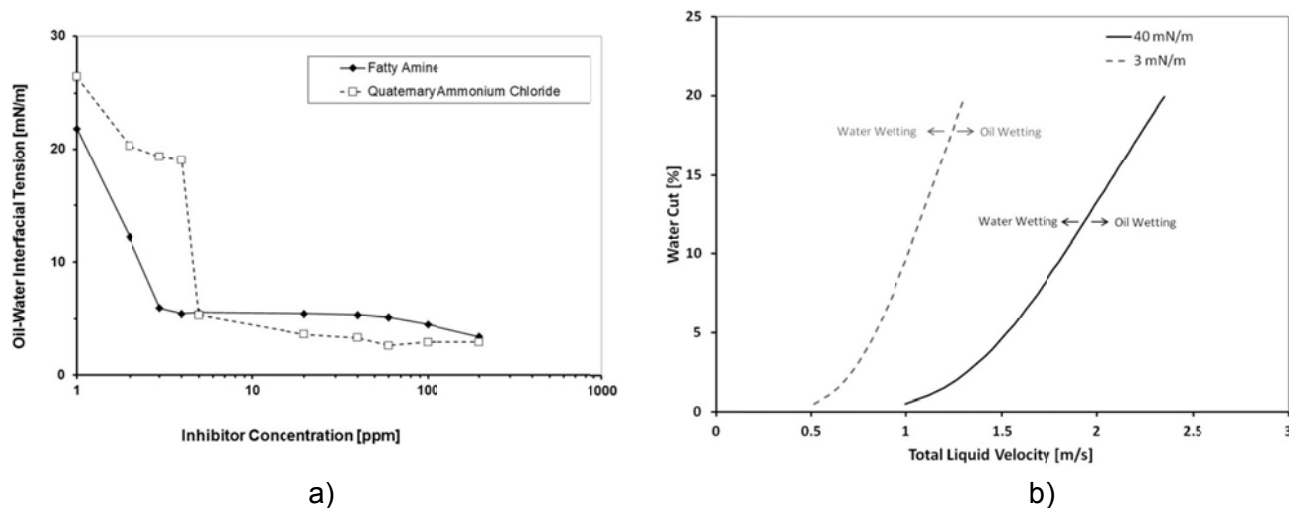


Figure 8: a) Interfacial tension of model oil and water with the addition of increasing concentration of inhibitor. b) Predicted transition between oil wetting and water wetting at high (40 mN/m) interfacial tension and low (3 mN/m) interfacial tension. Other oil properties were kept constant ($\rho=825 \text{ kg/m}^3$, $\mu=2.0 \text{ mPa}\cdot\text{s}$, $\theta=73^\circ$, $D=0.0555 \text{ m}$, $\beta=0^\circ$). On the right of the transition, oil wetting is predicted and on the left, water wetting is predicted.

By altering only the interfacial tension in the model and keeping the other required parameters constant it is possible to see the effect of the interfacial tension independent of other parameters. As can be seen in Figure 8b, by lowering the interfacial tension from 40 mN/m to 3 mN/m, the transition to oil wetting occurs at a much lower velocity. For instant, at 10% water cut, the transition occurs at 1.8 m/s when the interfacial tension is 40 mN/m, but at 1.1 m/s when the interfacial tension is 3 mN/m. The beneficial effects of corrosion inhibitors are not only to promote corrosion inhibition but also to keep the water entrained and away from the steel surface.

Contact Angle

The contact angle is a measurement of the static surface wettability. The oil-in-water contact angles for different concentration of fatty amine and quaternary ammonium chloride are shown in Figure 9a. The contact angle for a pure model oil is 22° (which denotes hydrophilic behavior) and with the addition of increasing concentration of fatty amine inhibitor, the contact angle increases rapidly, giving a hydrophobic contact angle ($>90^\circ$) with only 3 ppm concentration, which is the CMC for fatty amine.⁷ The contact angle does not increase as rapidly for quaternary ammonium chloride, and it does not become hydrophobic until the concentration has surpassed the CMC (which is 5 ppm for the quaternary ammonium chloride). Furthermore, the contact angle for the quaternary ammonium chloride is always lower than that of the fatty amine, reaching 125° at 200 ppm concentration, compared to 156° for fatty amine at the same concentration. This suggests that although the quaternary ammonium chloride does adsorb at the steel surface, it is not as efficient as fatty amine to form a hydrophobic layer.

The images incorporated into Figure 9a show how the higher contact angles correspond to the increasing spreading of the oil droplet on the steel surface. The increasing hydrophobicity of the steel surface with the addition of inhibitor is in contrast with the results of Foss, et al.²⁻⁴ With the exception of the oxidized (energized) surface,⁴ the water-in-oil contact angle measurement always gave a hydrophilic surface. The most plausible explanation for the difference between the Foss study and the current research is that in the current study the contact angle was measured with a freshly polished sample, while in the Foss study the sample was pre-corroded for 24 hours before the contact angle measurement was conducted.

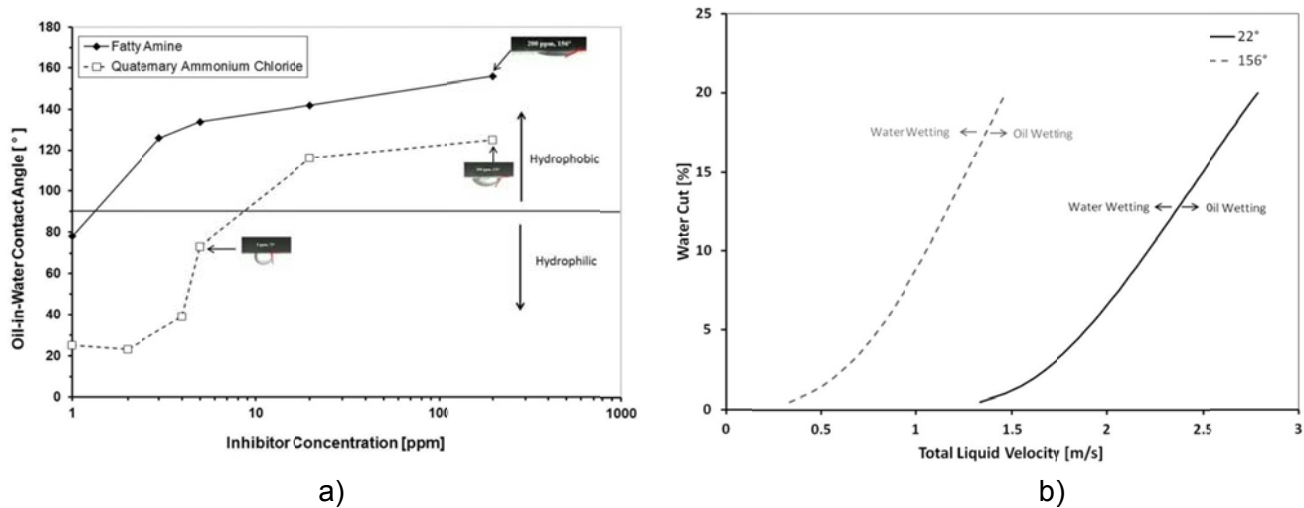


Figure 9: a) Oil-in-water contact angle for fatty amine and quaternary ammonium chloride. The images show the corresponding oil droplet. b) Predicted transition between oil wetting and water wetting at low (22°) contact angle and high (156°) contact angle. Other oil properties were kept constant ($\rho=825 \text{ kg/m}^3$, $\mu=2.0 \text{ mPa}\cdot\text{s}$, $\sigma=40 \text{ mN/m}$, $D=0.0555 \text{ m}$, $\beta=0^\circ$). On the right of the transition, oil wetting is predicted and on the left, water wetting is predicted.

It can be concluded that besides providing direct corrosion inhibition and increasing the likelihood of water entrainment, corrosion inhibitors can also provide corrosion protection by making the steel surface more hydrophobic and thereby facilitating oil wetting of the steel surface. The predicted transition from water wetting to oil wetting illustrating the effect of fatty amine, using the previously developed water wetting model⁹, can be seen in Figure 9b. It shows the transition as a function of the oil-in-water contact angle for a pure model oil water system (contact angle 22°) as well as the transition corresponding to the contact angle after an addition of 200 ppm of fatty amine into the water phase (156°). Higher contact angles make it easier to achieve oil wetting, in this case at 10% water cut the critical transition velocity is 2.3 m/s without the inhibitor, and is 1.4 m/s with 200 ppm of the inhibitor.

Doughnut Cell

The doughnut cell enables measurements of the dynamic wetting of the steel surface, which is rather different from the static wettability as measured by contact angles. The doughnut cell can provide data for constructing of a full phase wetting map, which displays the pattern of wetting as a function of water cut (%) and the flow velocity, as seen in Figure 10a for the model oil used here. There are three main wetting patterns detected, which are shown in Figure 10a:

- **oil wetting:** where all of the conductivity pins show oil wetted,
- **water wetting:** where at least some of the conductivity pins are permanently water wetted,
- **intermittent wetting:** where some of the conductivity pins are changing from oil to water wetting and vice versa.

The wetting map in Figure 10a shows that there is a threshold liquid velocity which needs to be reached before oil wet conditions are achieved and all the water is entrained. This threshold seems to increase as the water cut is increased, going from for example from 0.8 m/s for a 0.5% water cut to 1.9 m/s for a 20% water cut. The empirical transition line between oil wetting and intermittent wetting shown Figure 10a is considered to be the transition line from non-corrosive to corrosive conditions. A previous study⁸ showed that corrosion was not detected during oil wetting conditions and that the corrosion rate during intermittent wetting conditions was roughly half of the corrosion rate seen under full water wetting conditions.

©2013 by NACE International.

Requests for permission to publish this manuscript in any form, in part or in whole, must be in writing to NACE International, Publications Division, 1440 South Creek Drive, Houston, Texas 77084.

The material presented and the views expressed in this paper are solely those of the author(s) and are not necessarily endorsed by the Association.

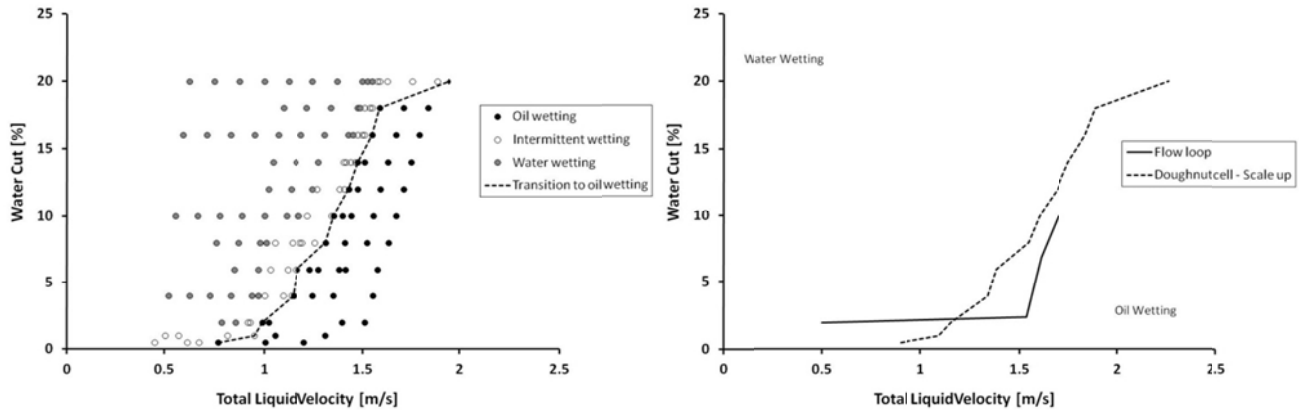


Figure 10: a) Phase wetting map for model oil ($\rho=825 \text{ kg/m}^3$, $\mu=2.0 \text{ mPa}\cdot\text{s}$, $\sigma=40 \text{ mN/m}$) made using the doughnut cell. The broken line shows the transition between oil wetting and non-oil wetting. b) comparison of the transition lines for model oil tested in the flow loop (full line) and the doughnut cell (broken line). In order to compare the transition lines directly for flow in two different geometries, the doughnut cell transition line has been scaled up using the water wetting model⁹.

There are a number of differences in the flow pattern achieved in the doughnut cell when compared to pipe flow:

- there is a difference in the shape of the cross section between the doughnut cell's rectangular channel and the circular cross section of a pipe;
- pipe flow is typically straight and the doughnut cell flow is circular;
- doughnut cell flow is shear driven while pipe flow is pressure driven, etc.

Despite all this the measured transition line to oil wetting is remarkably similar between the two measurement devices (doughnut cell vs. 4" ID flow loop) as can be seen in Figure 10b. Since the hydraulic diameter of the doughnut cell is roughly half the diameter of the flow loop, it was necessary to scale up the results of the doughnut cell to be able to compare them directly. The scale up is performed by using the previously developed water wetting model⁹, to isolate the effect of the diameter. Given the similarity between the benchtop scale doughnut cell data and the large scale flow loop results, it is confirmed that the doughnut cell can be used as an effective small scale, apparatus to study the surface wetting in horizontal oil-water flow.

The doughnut cell was used here to study how the surface wetting would change with the addition of an inhibitor. Figure 11 shows the empirical transition lines to oil wetting with the addition of quaternary ammonium chloride inhibitor. The oil wetted area becomes increasingly larger (*i.e.*, extends to lower liquid velocities) as the concentration of the inhibitor is increased. There is a large shift of the transition for concentrations up to the CMC (5 ppm). Increasing the inhibitor concentration above the CMC (up to 20 ppm) does not significantly alter the surface wetting since the surface is already saturated with the adsorbed inhibitor.

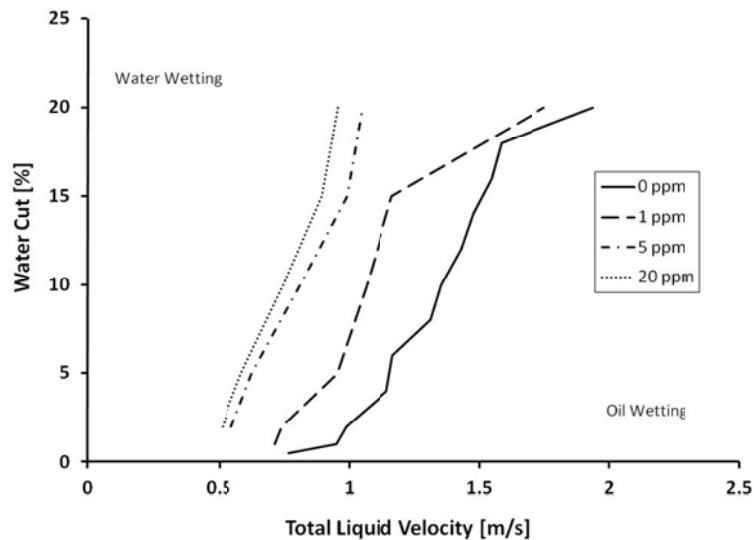


Figure 11: Transition from water to oil wetting with the addition of 1 ppm, 5 ppm and 20 ppm quaternary ammonium chloride in the doughnut cell.

CONCLUSIONS

- The measurements of the contact angle for the two generic inhibitors tested, suggest that the quaternary ammonium chloride does not form as strong an adsorption layer on the steel surface as the fatty amine does and is therefore not as effective in hindering access of water and dissolved corrosive species to the steel surface.
- Beyond lowering the corrosion rate, both inhibitors can lower the oil-water interfacial tension, making it easier for the water to be entrained in the oil flow.
- Both inhibitors can increase the oil wettability of the steel surface, making it harder for water to come into direct contact with the steel. This will decrease the likelihood of corrosion.
- The doughnut cell is a newly developed benchtop scale apparatus which can be used to simulate oil-water flow on a relatively small scale, saving both time and cost associated with large scale flow loop studies.
- The doughnut cell can provide measurements of the transition to oil wetting and it can be used to help optimize the inhibitor dosage in oil-water flow conditions.
- It was found that oil wetting did not increase significantly beyond the CMC concentration.

ACKNOWLEDGEMENTS

The authors would like to thank Albert Schubert, the Laboratory Director at the Institute for Corrosion and Multiphase Technology (ICMT) for assistance in the design of the doughnut cell. The financial support of the consortium of companies participating in the Water Wetting Joint Industry Project at ICMT, Ohio University is greatly appreciated. The companies are: BP, ConocoPhillips, ENI, ExxonMobile, Petrobras, Saudi Aramco, Shell and Total.

REFERENCES

1. McMahon, A. J., "The Mechanism of Action of an Oleic Imidazoline Based Corrosion Inhibitor for Oilfield Use," *Colloids and Surfaces*, 1991, 59(C), 187-208.
2. Foss, M., Gulbrandsen, E., Sjöblom, J., "Alteration of Wettability of Corroding Carbon Steel Surface by Carbon Dioxide Corrosion Inhibitors - Effect on Carbon Dioxide Corrosion Rate and Contact Angle." *Corrosion*, 2008, 64(12), 905-919.
3. Foss, M., Gulbrandsen, E., Sjöblom, J., "Effect of Corrosion Inhibitors and Oil on Carbon Dioxide Corrosion and Wetting of Carbon Steel with Ferrous Carbonate Deposits," *Corrosion*, 2009, 65(1), 3-14.
4. Foss, M., Gulbrandsen, E., Sjöblom, J., "Oil Wetting and Carbon Dioxide Corrosion Inhibition of Carbon Steel with Ferric Corrosion Products Deposits," *CORROSION*, 2010, 66(2), 025005-025005-11.
5. Schmitt, G. A.; Stradmann, N., "Wettability of Steel Surfaces at CO₂ Corrosion Conditions. I. Effect of Surface Active Compounds in Aqueous and Hydrocarbon Media," *CORROSION/98*, Paper no. 28 (Houston, TX: NACE International, 1998).
6. Yang, S., Robbins, W., Richter, S., Nescic, S., "Evaluation of the Protectiveness of Paraffins for CO₂ Corrosion," *CORROSION/12*, Paper no. C2012-0001323, (Houston, TX, NACE International, 2012).
7. Li, C. "Effect of Corrosion Inhibitor on Water Wetting and Carbon Dioxide Corrosion In Oil-Water Two Phase Flow", Dissertation, Ohio University, Athens, OH, 2009.
8. Cai, J., Li, C., Tang, X., Ayello, F., Richter, S., Nescic, S., "Experimental Study of Water Wetting in Oil-water Two Phase flow—Horizontal Flow of Model Oil," *Chemical Engineering Science*, 2012, 73(0), 334-344.
9. Tang, X., Richter, S., Nescic, S., "A New Improved Model for Phase Wetting Prediction in Oil-Water Two Phase Flow," *Corrosion/2013*, Paper no. C2013-0002393 (Houston, TX, NACE International, 2013).